Ionizing radiation improves RIG-I mediated immunotherapy through enhanced p53 activation in malignant melanoma

Silke Lambing[a], Stefan Holdenrieder[a,c], Patrick Müller[a], Christian Hagen[a], Stephan Garbe[b], Martin Schlee[a], Jasper G. van den Boorn[a], Eva Bartok[a,d], Gunther Hartmann[a*] and Marcel Renn[a,e*]

[a] Institute of Clinical Chemistry and Clinical Pharmacology, University Hospital Bonn, Bonn, Germany

[b] Department of Radiation Oncology, University Hospital Bonn, Bonn, Germany

[c] Institute of Laboratory Medicine, German Heart Centre, Munich, Germany

[d] Unit of Experimental Immunology, Department of Biomedical Sciences, Institute of Tropical Medicine, Antwerp, Belgium

[e] Mildred Scheel School of Oncology, Bonn, University Hospital Bonn, Medical Faculty, D-53127, Bonn, Germany

* denotes shared authorship.

The activation of the innate immune receptor RIG-I is a promising approach in immunooncology and currently under investigation in clinical trials. RIG-I agonists elicit a strong immune activation in both tumor and immune cells and induce both direct and indirect immune cell-mediated tumor cell death which involves tumor-specific cytotoxic T-cell response and type I interferon-driven innate cytotoxic immunity. Besides RIG-I, irradiation is known to induce cytotoxic DNA damage resulting in tumor debulking followed by the induction of tumor-specific immunity. To date, it is unclear whether the molecular antitumor effects of RIG-I and irradiation are additive or even synergize. Here, we investigated the combination of RIG-I activation with radiotherapy in melanoma. We found that low dose x-ray irradiation enhanced the extent and immunogenicity of RIG-I mediated tumor cell death in human and murine melanoma cell lines and in the murine B16 melanoma model *in vivo*. Pathway analysis of transcriptomic data revealed a central role for p53 downstream of the combined treatment, which was corroborated using $p53^{-/-}$ B16 cells. *In vivo*, the additional effect of irradiation on immune cell activation and inhibition of tumor growth was lost in mice carrying p53-knockout B16 tumors, while the response to RIG-I stimulation in those mice was maintained. Thus, our results identify p53 as pivotal for the synergy of RIG-I with irradiation, resulting in potent induction of immunogenic tumor cell death. Consequently, low dose radiotherapy holds great promise to further improve the efficacy or RIG-I ligands especially in patients with malignant melanoma or other tumors exhibiting a functional p53 pathway.

Introduction

Recent advances in immunotherapy have significantly prolonged survival for patients with many types of tumors [1]. In addition to immune checkpoint inhibition, targeted stimulation of the innate immune system has become the focus of a number of preclinical and clinical studies [2,3]. One particularly promising approach is the specific activation of the cytosolic RNA receptor RIG-I, which is under investigation as a single therapy or in combination with pembrolizumab (NCT03739138) for the treatment of solid tumors.

RIG-I is a cytosolic antiviral receptor that recognizes 5'-tri- or 5'-diphosphate, blunt-ended double-stranded RNA [4–6]. In addition to its ability to trigger a potent innate cytotoxic immune response, RIG-I stimulation has the ability to directly induce tumor cell death [7,8]. This RIG-I-induced cell death bears the hallmarks of an immunogenic cell death [9], such as HMGB1 release and calreticulin exposure on the cell surface [10–12]. RIG-I stimulation *in situ* thus possesses features of a cancer vaccine: it can turn a cold tumor into a hot tumor that simultaneously releases tumor antigens and creates a pro-immunogenic environment facilitating the development of tumor-specific cytotoxic T cells [10,13].

Radiation therapy is also a well-known inducer of immunogenic tumor cell death [14]. Irradiated, dying tumor cells have been reported to release pro-inflammatory cytokines including CXCL16 and TNFα [15,16], the cGAS ligand cGAMP [17,18], and alarmins such as HMGB1 and ATP [19–21]. There have also been reports that ionizing radiation (IR) can induce the expression of MHC class I proteins [22,23] and calreticulin [24,25] on the surface of irradiated, dying cells, which promotes recognition and internalization of the cells by phagocytes and subsequent T cell activation. In recent studies, radiation has been combined with immunotherapies such as checkpoint inhibitors in pre-clinical and clinical trials [26]. For example, high-dose (20 Gy) radiation enhanced the efficacy of antibodies against CTLA4 or PD-L1 in the B16 mouse melanoma model [27] and in a phase I/II trial, fractionated radiotherapy improved the survival of non-small-cell lung cancer patients co-treated with pembrolizumab (anti-PD-1) compared to pembrolizumab alone [28]. However, therapies that combine irradiation and targeted innate immune activation have not yet been widely explored, and there is no information to date about the combination of irradiation and specific activation of RIG-I.

In the current study, we investigated the effect of a combination therapy between the RIG-I ligand 3pRNA and low-dose (2 Gy) irradiation. Irradiation significantly increased RIG-I-induced immunogenic cell death in both human and murine melanoma cell lines and tumor-cell uptake and activation of dendritic cells. Using an *in vivo* B16 melanoma model, we observed that cotreatment of 3pRNA with low-dose, tumor-targeted irradiation resulted in increased activation of T- and NK cells in draining lymph nodes and prolonged the overall survival of tumor-bearing animals. Pathway analysis of transcriptomic data revealed a central role for p53 downstream of the combined treatment, which was corroborated using $p53^{-/-}$ B16 cells. Here, we found that, while the contribution of RIG-I was independent of p53, the additional effect of irradiation was indeed p53-dependent. Altogether, our study demonstrates that radiotherapy could potentially enhance RIG-I-mediated immunotherapy, especially in patients with tumors with an intact p53 pathway, such as most malignant melanomas.

Results

Combined 3pRNA radio-immunotherapy induces immunogenic tumor cell death and tumor cell uptake by dendritic cells as well as activation in vitro

To investigate whether irradiation combined with RIG-I activation has a synergistic effect on the induction of immunogenic cell death *in vitro*, we stimulated the murine B16 and human A375 melanoma cell lines with the RIG-I ligand 3pRNA [29] followed by 2 Gy of ionizing radiation (IR) 30 min later. Irradiation significantly increased RIG-I-induced cell death, as measured by Annexin V positive and Annexin V/7AAD double-positive cells (Fig. 1 A-B, suppl. Fig. 1 A) as well as intracellular cleaved caspase 3 levels (suppl. Fig. 1 C). Moreover, RIG-I activation and irradiation significantly lowered the EC_{50} for the induction of cell death as quantified by Annexin V/7AAD staining, from 987 ng/ml for 3pRNA alone to 293 ng/ml of 3pRNA in combination with 2 Gy radiation in murine B16 cells and from 1754 ng/ml to 333 ng/ml in human A375 melanoma cells (Fig. 1 C, D, suppl. Fig. 1 D, E). Since higher radiation doses increased cell death on their own but did not further increase RIG-I-induced melanoma cell death (suppl. Fig. 1 F), a radiation dose of 2 Gy was used throughout the rest of the study. Several other human melanoma cell lines (MaMel19, MaMel54, and MaMel48) and A549 lung adenocarcinoma cells also showed increased cell death when RIG-I stimulation was combined with irradiation (Fig. 1 E, F). Notably, this effect could not be recapitulated with the addition of recombinant IFN-α alone (suppl. Fig. 1 B).
Calreticulin exposure on the outer leaflet of the cell membrane induces efferocytosis of dead or dying cells by antigen presenting cells (APCs) and is a hallmark of immunogenic cell death [30]. In agreement with the Annexin V data, calreticulin exposure was also found to be significantly increased when irradiation and RIG-I activation were combined in murine B16 melanoma cells and human A375 cells (Fig. 1 G, H). Surface expression of calreticulin was highest in Annexin V/7AAD double-positive cells, which are known to be in late-stage programmed cell death (suppl. Fig. 1 G). Interestingly, the expression of MHC-I on murine B16 cells and human A375 melanoma cells was also strongly induced by the combination treatment, most prominently on Annexin V/7AAD negative cells (suppl. Fig. 1 G, H, I). Furthermore, the release of the nuclear protein HMGB1, which serves as a danger-associated molecular pattern (DAMP) and is another characteristic of immunogenic cell death, was induced by RIG-I stimulation in both cell lines and further increased by 2 Gy irradiation in human A375 cells (Fig 1 I, J). RIG-I stimulation, but not 2 Gy irradiation, induced the release of type I interferon in murine B16 melanoma cells and type I and type III interferon in human A375 cells. In murine B16 cells, combination treatment slightly enhanced the secretion of IL6 and TNFα but did not lead to an increase in the release of interferons or the interferon-stimulated chemokine CXCL10 (suppl. Fig. 2 A), whereas in human A375 cells, IL6, GMCSF, IL29 (interferon lambda 1) and CXCL10, but not IFN-β was enhanced by irradiation when added to RIG-I stimulation (suppl. Fig. 2 B).
To test whether the combination treatment had an impact on tumor-cell uptake by professional antigen-presenting cells and their activation, B16 melanoma cells were treated as before with 3pRNA and irradiation, but then stained with the eFluor780 fixable live/dead dye and co-incubated with bone marrow-derived dendritic cells (BMDCs). BMDCs of wildtype C57BL/6 mice “fed” with B16 cells after combination treatment demonstrated higher levels of eFluor780 dye uptake than after irradiation or RIG-I activation alone. Combination treatment also significantly enhanced the expression of the costimulatory molecule CD86 and the immune cell activation marker CD69 (Fig. 1 K).

3pRNA antitumor immunotherapy in vivo is enhanced by low-dose irradiation

Next, we studied combined irradiation and RIG-I activation *in vivo*. C57BL/6 mice with palpable subcutaneous B16 melanoma were treated with 2 Gy precision irradiation of the tumor area and intratumoral injection of 20 µg 3pRNA twice a week. Compared to untreated tumors, both 3pRNA treatment and irradiation alone prolonged the survival of the mice. The combination of irradiation and RIG-I activation resulted in the longest overall survival (Fig. 2 A). In tumor-draining lymph nodes analyzed at 16 hours after treatment, NK cells and $CD8^+$ T cells showed increased expression of the activation marker CD69 upon RIG-I activation, with highest expression when RIG-I activation and irradiation were combined. In $CD4^+$ T cells, only the combination treatment of RIG-I activation and irradiation induced significant upregulation of CD69 (Fig. 2 B).

Transcriptomic analysis of melanoma cells after combination therapy reveals activation of the p53 signaling pathway

To explore the potential molecular mechanisms of the combination therapy, we performed whole-genome transcriptional analysis with an Affymetrix gene chip on B16.F10 cells six hours after treatment with 3pRNA and irradiation. Upon RIG-I stimulation, we observed a strong change in gene-expression patterns and the robust induction of interferon stimulated genes (ISGs), whereas irradiation primarily induced genes associated with the DNA damage response (Fig 3 A). As expected, a pathway analysis of differentially expressed genes showed that RIG-I stimulation was associated with pathways involved in innate immunity, while irradiation induced genes of the p53 pathway. The p53 pathway was also among the most significantly upregulated pathways in the combination group (Fig. 3 B) and the only differentially regulated pathway between RIG-I activation alone and its combination with irradiation (Fig. 3 C, D). Given the central role of p53 signaling in DNA damage and cell-cycle control, we reasoned that it may also be involved in the synergistic antitumoral effects observed for the combination treatment.

Combined irradiation and RIG-I activation synergistically induces p53 signaling and prolongs cell-cycle arrest

We then examined the effect of RIG-I activation, irradiation and combination treatment on p53 phosphorylation and signaling. As expected, irradiation induced p53 phosphorylation six hours after treatment, which declined after 24 hours. In contrast, RIG-I activation alone only led to weak p53 phosphorylation and only after 24 hours. However, combination treatment with 3pRNA and irradiation caused B16 cells to retain strong p53 phosphorylation even 24 hours after treatment (Fig. 4 A). Notably, total p53 protein levels at 24 hours were only elevated in 3pRNA-transfected B16 cells (both with and without irradiation). Moreover, these effects were not seen when irradiation was combined with control RNA or IFNα. We then analyzed two proteins induced by p53, Puma (Fig. 4 A) and p21(Fig. 4 B). Puma was induced by RIG-I activation and irradiation both at six hours and 24 hours, with the strongest signal in the combination group at 24 hours (Fig. 4 A). p21 was upregulated 24 hours after RIG-I stimulation or irradiation and most strongly in combination, while ATM, an important upstream regulator of p53 activation, was only upregulated by RIG-I stimulation and not further upregulated by combination treatment (Fig. 4 B).
To monitor cell-cycle progression, we stained B16 melanoma cells with propidium iodide six, 12, and 24 hours after 2 Gy irradiation and RIG-I stimulation. Irradiation induced a G2/M cell-cycle arrest after six hours which was already less pronounced after 12 hours and had completely resolved 24 hours post-irradiation (Fig. 4 C). RIG-I stimulation alone, on the other hand, led to a G1/S arrest, which took 24 hours to develop, in line with its slower induction of p53 phosphorylation when compared to irradiation (Fig. 4 A). Like irradiation alone,

combination of irradiation and RIG-I stimulation led to a G2/M arrest after six hours. However, this arrest was maintained even after 24 hours (Fig. 4 C), which was consistent with the time course observed for p53 phosphorylation (Fig. 4 A).

Synergistic effect of irradiation and RIG-I activation is p53 dependent, while the RIG-I effect alone is p53 independent

To test the functional relevance of p53 in combination therapy, we generated polyclonal p53-knockout (KO) cells using Crispr/Cas9 genome editing. Polyclonal $p53^{-/-}$ B16 and $p53^{-/-}$ A375 melanoma cells showed no basal p53 expression and, as expected, did not upregulate p53 protein at two hours nor the p53 target protein p21 at 24 hours following irradiation (Supp. Fig. 3 A-D). While the amount of cell death induced by 3pRNA treatment alone was similar between wildtype and knockout cells, the increase upon additional irradiation was largely abolished in the $p53^{-/-}$ cells (Fig. 5 A, B). Correspondingly, no contribution of irradiation to cell death induction was observed in human p53 deficient SK-Mel28 melanoma cells, which carry an endogenous inactivating p53 mutation [31] (Supp. Fig. 3 E). Nevertheless, RIG-I stimulation still induced strong cell death in those SK-Mel28 melanoma cells despite the lack of functional p53 [31] (Supp. Fig. 3 E). Similar to the induction of cell death, the G1/S arrest induced by RIG-I stimulation alone after 24 hours was still present in the p53 KO B16 melanoma cells. Furthermore, the G2/M arrest induced by irradiation after six hours was still detectable, but the prolonged G2/M arrest after 24 and 48 hours with combination treatment was absent in the p53 KO cells (Fig. 5 C).
Analysis of single phases of the cell cycle revealed that the highest proportion of cells were in G2/M phase arrest after 48 hours, which, at this time point, only occurs after combination treatment in wildtype cells but not p53 deficient cells (Supp. Fig. 4). Moreover, the observed correlation of G2/M cell cycle arrest (Fig 5 B) and caspase 3 activity (Supp. Fig. 4) underscores the close link between cell cycle arrest and cell death.
Calreticulin expression on the cell surface of p53-deficient murine B16 or p53 deficient human A375 melanoma cells was not further enhanced by combining RIG-I stimulation with irradiation (Fig. 5 D, E). Corresponding to the level of cell-surface calreticulin, the effect of irradiation on the uptake of p53 KO B16 melanoma cells was markedly reduced in comparison to wildtype cells. Furthermore, no irradiation-dependent increase in the expression of the activation markers CD86 und CD69 on dendritic cells could be detected when the phagocytosed tumor cells lacked p53 (Fig. 5 F). This shows that all irradiation-dependent effects, including cell death, immunogenicity, subsequent uptake of dying cells by DCs, and activation of DCs, are dependent on the expression of p53 in melanoma cells, whereas the effect of RIG-I treatment alone is not affected by the absence of p53.

Synergistic anti-tumor activity of irradiation and RIG-I, but not the effect of RIG-I alone, in vivo depends on functional p53 in melanoma

In the B16 melanoma model *in vivo*, both T cell activation and NK cell activation in the draining lymph node, as measured by upregulation of CD69 on $CD8^+$ T cells, $CD4^+$ T cells and $NK1.1^+$ NK cells was significantly enhanced by 3pRNA injection compared to untreated mice. Additional irradiation of the tumor area further enhanced the expression of activation markers on T cells and NK cells in the draining lymph nodes. This additional irradiation-dependent stimulatory effect was lost in mice which were challenged with p53-deficient tumor cells (Fig. 6 A), recapitulating the results obtained for immunogenic cell death and dendritic cell activation *in vitro* (Fig. 5 and suppl. Fig. 3). Consistent with activation of T cells and NK cells in draining lymph nodes, tumor growth was significantly reduced by RIG-I stimulation in wildtype and p53 KO melanomas, but the significant additional effect of local

tumor irradiation was reduced and no longer statistically significant when mice were challenged with p53 deficient melanoma cells (Fig. 6 B). This further supports the notion that the synergistic effect of combination treatment *in vivo* is dependent on p53 expression within the tumor cell. Nonetheless, the effectivity of RIG-I immunotherapy itself was independent of the p53 status of the melanoma cells.

Discussion

Several studies in different tumor models have demonstrated that intratumoral injection of RIG-I ligands induces an effective anti-tumor immune response [8,32], and this immunotherapeutic strategy is currently being explored in clinical trials (NCT03739138). However, intratumoral injection of RNA ligands remains technically challenging and limited by injection volumes and the concentration of RNA in delivery systems [33].

Here, we found that combination of RIG-I treatment with radiotherapy is a highly promising combinatorial treatment for tumors with intact p53 pathway, such as most malignant melanomas [34]. Localized irradiation of the tumor in a melanoma model *in vivo* substantially improved therapeutic efficacy of intratumoral RIG-I ligand injections. This enhanced anti-tumor effect was accompanied by increased activation of $CD4^+$ and $CD8^+$ T cells and of NK cells in tumor-draining lymph nodes. *In vitro*, low-dose ionizing irradiation of tumor cells synergistically enhanced RIG-I-mediated induction of immunogenic tumor cell death as characterized by increased cell-surface expression of calreticulin and the release of HMGB1 and of inflammatory chemokines and cytokines. The uptake of such immunogenic cell death material by dendritic cells enhanced their activation status. Molecularly, the synergy of irradiation and RIG-I could be ascribed to distinct effects on the p53 pathway, resulting in a prolonged cell cycle arrest of tumor cells in the G2/M phase, which only occurred if RIG-I and irradiation were combined, leading to subsequent immunogenic cell death. Notably, the p53 pathway was required for synergistic activity *in vitro* and *in vivo* but not for the anti-tumor activity of intratumoral RIG-I ligand treatment as a single treatment.

P53 is one of the most important tumor-suppressor genes. In approximately 50% of all human tumors, p53 is either mutated or functionally inactive [35] or Mdm2 is overexpressed and downregulates p53 expression [36]. Therefore, the data in our study that demonstrate the p53-independence of RIG-I therapy as a monotherapy are encouraging for RIG-I-mediated immunotherapy in general. Based on our results, the combination of RIG-I with radiotherapy should be limited to tumors with an intact p53 pathway. In melanoma the frequency of p53 mutations is only 10 to 19% [34], suggesting that the combination therapy is well suited for malignant melanoma as a target tumor entity.

It is interesting to note that there is evidence from previous studies that p53 signaling is important to antiviral defense and interferon signaling [37,38]. It has been shown that treatment with IFN-β concurrent to irradiation or chemotherapy in mouse embryonic fibroblasts and in human hepatic cancer cells IFN-β sensitized the cells for a higher induction of apoptosis [38]. However, in our study, recombinant type I IFN was not a sufficient substitute for RIG-I stimulation since it did not co-trigger enhanced and prolonged p53 phosphorylation or the induction of immunogenic cell death by radiotherapy.

In one study, the combination of irradiation and innate immune activation was studied in lung carcinoma cell lines, where the unspecific antiviral receptor agonist poly(I:C) together with 4 Gy irradiation was demonstrated to enhance the cytotoxic effects of the monotherapies on carcinoma cell lines in a caspase-dependent manner *in vitro* [39]. However, it should be noted that poly(I:C) activates multiple dsRNA receptors, including PKR, OAS1, ZBP1, TLR3, MDA5, and RIG-I (Bartok and Hartmann, 2020), rendering this rather non- specific immunotherapeutic approach more prone to interindividual variability and immunotoxic side effects.

Another study has demonstrated synergistic inhibition of tumor growth and enhanced induction of long-term immune memory cells in murine mammary and pancreatic carcinoma models using a combination of poly(I:C) injection with transplantation of alpha-emitting radiation seeds into the tumor [40], an experimental treatment approach that is currently tested in clinical trials (e.g., NCT-04377360, NCT-03353077, NCT-03015883). In contrast, in our approach, a clinical linear accelerator has been used, which is standard clinical practice and is therefore directly applicable in routine clinical care.

Another interesting aspect of irradiation and immunity is that localized irradiation by itself, independent of additional innate immune activation, has been shown to improve tumor infiltration of adoptively transferred T cells in a pancreatic cancer model [41]. With regard to irradiation intensity, other studies have shown that low doses (2–8 Gy) of irradiation elicit stronger antitumor immunity compared to high doses, especially when given repetitively or when combined with other antitumoral treatments [24,42,43]. In our study, despite the modest antitumoral response induced by 2 Gy irradiation alone, this low dose turned out to be more advantageous at co-activating RIG-I-mediated immunity than higher doses of 5 and 10 Gy.

Altogether, our study clearly demonstrates that combining the DNA-damaging treatment radiotherapy with RIG-I innate immune signaling synergistically boosts p53-dependent immunogenic tumor-cell death, further underscoring the rationale for evaluating a localized combination therapy that turns cold into hot tumors as an *in situ* cancer vaccine [13]. Since melanoma is classically considered a “radioresistant” tumor, our study also provides a new rationale for reevaluating radiotherapy in combination with RIG-I activation for a broad range of oncological indications. Moreover, as with other synergistic treatments, it could potentially allow for a reduction of the individual radiation doses and thus reduce the severe side effects associated with radiotherapy.

Material & Methods

Cell lines

Human A375 and SKmel28 melanoma cells, human lung adenocarcinoma cells A549, murine B16.F10 melanoma cells were cultured in DMEM and human melanoma cells MaMel19, MaMel54, and MaMel48 were cultured in RPMI 1640 both supplemented with 10% heat-inactivated fetal bovine serum (FCS), 100 IU/ml penicillin, and 100 µg/ml streptomycin (all from Thermo Fisher Scientific) in a humidified incubator at 37°C and 5% CO_2. A375 cells were kindly provided by Michael Hölzel (University Hospital Bonn, Germany) and MaMel19, MaMel54 and MaMel48 were kindly provided by Jennifer Landsberg (University Hospital Bonn, Germany) and Dirk Schadendorfer (University Hospital Essen, Germany). B16 and SKmel28 were purchased from ATCC. Identity of human cell lines was confirmed by short-tandem-repeat (STR) profiling (Eurofins). Cells were checked monthly for mycoplasma infection by testing the supernatant with the reporter cell line of the Mycoplasma Detection Kit "PlasmoTest" from Invivogen.

Oligonucleotides, reagents and chemicals

5'-triphosphorylated double-stranded RNA (3pRNA) were *in vitro* transcribed (IVT) from a DNA templateby using the phage T7 polymerase from the Transcript Aid T7 high-yield Transcription Kit (Fermentas) as described previously [29]. Inert AC_{20} control RNA (5'-CACAACAAACCAAACAACCA-3') was obtained from Biomers. Murine IFNα was purchased from BioLegend. The MDM2 inhibitor AMG232 was purchased from MedChemExpress.

Oligonucleotide-transfection of tumor cells

Cells were seeded at a defined cell number the day before transfection and cultured overnight at 37°C and 5% CO_2 in an incubator to ensure proper attachment. Lipofectamine 2000 (Invitrogen) and OptiMem (Thermo Fisher Scientific) were used according to the manufacturer's protocol to transfect control AC_{20} RNA or stimulatory 3pRNA at the indicated concentrations.

Irradiation of tumor cells

Cells were irradiated with high-energy photons (150 keV) of 2 Gy generated by a biological irradiator (RS-2000, Rad Source Technologies).

DC melanoma uptake

Bone-marrow derived dendritic cells were generated as described previously [44]. B16 melanoma cells were stimulated as indicated. After 48 h melanoma cells were stained with eFluor780 fixable viability dye (eBioscience, 1:2000 in PBS) for 30 min on ice. Excess dye was washed away by the addition of DMEM supplemented with 10% FCS. Stained melanoma cells (25 000) were then cocultured with 10 0000 bmDCs overnight at 37°C and 5% CO_2 in a 96well plate. The next day, DCs were detached by adding 2 mM EDTA/PBS and analysed by flow cytometry.

Generation of polyclonal p53 knockout (KO) cell lines by using CRISPR/Cas9

The CRISPR target site for murine p53 (single guide (sg) RNA: 5´-CTGAGCCAGGAGACATTTTC-3´) was already cloned into a px330 plasmid (px330-U6-Chimeric_BB-CBh-hSpCas9, Addgene plasmid #42230) and for human p53 (sgRNA: 5´-GCATCTTATCCGAGTGGA-3´) was already cloned into a px459 plasmid (pSpCas9(BB)-2A-Puro (px459) V2.0 (Addgene plasmid #62988)) and kindly provided by Daniel Hinze from the lab of Michael Hölzel. B16 and A375 cells were seeded at a density of $5x10^4$ cells per well into a 12-well plate the day before transfection with 2 µg of the CRISPR/Cas9

plasmid using Lipofectamin 2000. After three days of incubation at 37°C, the transfected cells were seeded out again into 12-well plates at a density of $5x10^3$ cells per well. One day later 10 µM of the MDM2 inhibitor AMG232 was added to the culture medium for five days to positively select p53 deficient cells.

Gene-expression analysis with microarray

B16.F10 cells were transfected with 50 ng/ml 3pRNA or AC_{20} control RNA and irradiated with 2 Gy or not for 6 h. RNA was isolated with the RNeasy Mini Kit (Qiagen) according to the manufacture's instructions. The extracted RNA was further processed using an Clariom S Mouse Genchip (Thermo Fisher) at the LIFE & BRAIN Genomics Service Center Bonn.

Western blot analysis

Total cell protein extraction was done as described previously [45]. 30–50 µg of protein was mixed with an equal amount of 2x Laemmli buffer (200 mM Tris/HCl pH 6.8, 4% SDS, 20% glycerol, 200 mM DTT), denatured at 95°C for 5 min, separated by SDS gel electrophoresis (30 mA per gel, 1.5 h), and transferred onto a nitrocellulose membrane (GE Healthcare, 0.45 µm pore size of the membrane). Proteins were transferred using 450 mA for 1.5 h. The membranes were blocked with 5% non-fat dry milk in TBST buffer (150 mM NaCl, 20 mM Tris, 0.1% Tween 20, pH 7.6) for 1 h at room temerature (RT) and incubated with the respective primary antibodies at 4°C overnight (anti-phospho-p53 (Ser15), anti-p53, anti-puma, anti-p21 (all 1:1000, Cell Signaling);). HRP-coupled secondary antibodies, anti-rabbit and anti-mouse (Cell Signaling), were used 1:5000 or IRDye800 coupled anti-rabbit and anti-mouse (Li-cor Bioscience) antibodies were used 1:10,000 in 5% milk/TBST and incubated for 1 h at RT. Anti-actin-HRP antibody (Santa Cruz) diluted 1:5000 in 5% milk/ TBST or mouse/rabbit anti-ß-actin (Li-cor Bioscience) diluted 1:10,000 was used to detect actin as a loading control. Protein bands were detected by using chemiluminescence of an ECL western-blotting substrate (Thermo Scientific) or by near-infrared fluorescence with the Odyssey Fc (Li-cor Biosciences).

Enzyme-linked immunosorbent assay (ELISA)

To determine concentrations of HMGB1, the supernatants were collected 24 h after transfection and irradiation of tumor cells and the HMGB1 ELISA Kit from IBL International was used according to the manufacturer's protocol.

Flow cytometry

Cells of interest were harvested with trypsin and washed with PBS. For staining of surface proteins, fluorochrome-conjugated monoclonal antibodies were diluted 1:200 in FACS buffer (1x PBS containing 10% FCS, 2 mM EDTA and 0.05% sodium azide) and incubated with the cells 15–20 min on ice or RT. Antibodies used: APC-Cy7 or BV510 anti-CD4, PerCP-Cy5.5 or BV421 anti-CD8, PerCP anti-CD45, BV421 anti-CD11c, Alexa-Fluor-488 or BV510 anti-CD69, BV785 anti-CD86, BV785, BV510 anti-MHC-I (Hk2b), FITC anti-I-A/E (all BioLegend), FITC anti-CD11c, APC anti-MHC-I (Hk2b), PE or BV650 anti-NK1.1 (all eBioscience), BUV737 anti-CD4, BUV395 anti-CD8, BUV395 anti-CD11b, FITC anti-HLA ABC (all BD Bioscience), Alexa-488 anti-Calreticulin (Cell Signaling Technology, 1:100 instead of 1:200).

For *in vivo* studies, the tissue was digested with 1 mg/ml collagenase D in PBS with 5% FCS for 20 min at 37°C and afterwards passed through a 70 µm cell strainer with sterile PBS. Cells were afterwards stained with Zombie UV fixable viability stain (1:500 in PBS, BioLegend for 20 min at RT followed by blocking of Fc receptors (Anti-Mouse CD16/32 from eBioscience, 1:200 in FACS buffer) for 15 min on ice. Surface staining was performed as described above.

Intracellular staining of activated, cleaved caspase-3 was analyzed using a rabbit anti-cleaved caspase-3 monoclonal antibody (1:500, Cell Signaling Technology) followed by a second staining with FITC-anti-rabbit IgG (1:200, BioLegend). Both antibodies were diluted in FACS buffer supplemented with 0.5% saponin.

Fluorescence intensities for all of the flow cytometry-based assays were measured with the LSRFortessa flow cytometer (BD Biosciences), or with the Attune NxT Flow Cytometer (Thermo Fisher).

Quantification of apoptotic cell death

Cells were stained with anti-Annexin V-Alexa 647 antibody or anti-Annexin V-Pacific Blue antibody (both 1:30, BioLegend) in Annexin binding buffer (10 mM HEPES, pH 7.4; 140 mM NaCl; 2.5 mM $CaCl_2$) and incubated at RT for 20 min in the dark. Cells were washed and resuspended in 200 µl 1x binding buffer. 5 µl of 7-amino-actinomycin D (7AAD, 50 µg/ml working solution in PBS, Thermo Fisher Scientific) was added to the stained cells 5–10 min before measurement.

Multiplex cytokine assay

Multiplex flow-cytometric cytokine detection was performed on cell-culture supernatants collected 24 h after 3pRNA transfection and irradiation. Cytokine levels were measured using human and mouse LEGENDplex bead-based multi-analyte flow assay kits as described in the manufacturer's manual. However, the assay was performed in a 384 well plate and the volumes adjusted accordingly.

Cell-cycle-phase analysis

Anaylsis of the cell-cycle phases was performed on cells that were fixed and permeabilized with 70% ethanol for one hour at RT. Cells were incubated for 30 min at RT with 10 µg/ml propidium iodide (PI) and 100 µg/ml RNase A in FACS buffer, and directly analyzed by flow cytometry. For simultaneous staining of activated caspase 3, the cultivation medium of cells seeded in 96-well plates was exchanged for 50 µl/well of staining solution, containing CellEvent Caspase3/7 Green ReadyProbes, according to the manufacturer's protocol, and 100 µg/ml Hoechst 33342 (both Thermo Fisher Scientific) and incubated for 30–60 min at 37°C. The cells were then detached and analyzed by flow cytometry.

***In vivo* studies with mice**

Female C57BL/6 mice were obtained from Janvier and used at 8–12 weeks of age. The animals were housed in individually ventilated cages (IVC) in the House of Experimental Therapy (HET) at the University Hospital Bonn. All experiments were approved by local- and regional animal ethics committees. Mice were injected with 1×10^5 B16.F10 cells in 100 µl sterile PBS subcutaneously into the right flank of the back. When the tumors reached a diameter of 3–4 mm, the tumors were injected with 20 µg 3pRNA or AC_{21} single-stranded control RNA complexed with JetPEI (Polyplus) according to the manufactorers protocol and afterwards locally irradiated with a single dose of 2 Gy. For local irradiation, the mice were narcotized and positioned in the treatment beam. The tumors were stereotactically irradiated with adapted field size in a range between 1 - 2 cm using a linear accelerator with a 6 MeV beam (TrueBeam STx, Varian and Mevatron MD, Siemens). The mice were surrounded by water-equivalent RW3 sheets (PTW, Freiburg) and placed in the depth-plane Dmax (15 mm) of the 6 MeV-Beam. For the survival studies, treatment of the tumor with 3pRNA/AC_{20} RNA was repeated twice a week and tumor size was measured daily until the tumors reached a diameter of 10 mm.

Statistical analysis

If not indicated otherwise, data are represented as the mean +/- SEM of at least three experiments that were run with two replicates per sample and a statistical analysis of the difference between groups using one or two-way ANOVA, as appropiate, calculated with GraphPad Prism 8. * ($P < 0.05$), ** ($P < 0.01$), *** ($P < 0.001$), **** ($P < 0.0001$), ns: not significant.

Declarations

Ethics approval and consent to participate

All animal experiments were approved by the local authorities (LANUV NRW).

Funding

This study was funded by the Deutsche Forschungsgemeinschaft (DFG, German Research Foundation) under Germany s Excellence Strategy EXC2151 390873048 of which E.B., G.H., and M.S. are members. It was also supported by the Deutsche Forschungsgemeinschaft (DFG, German Research Foundation) Project-ID 369799452 TRR237 to E.B., G.H., and M.S, SFB670 to E.B., G.H., and M.S., SFB704 to G.H., GRK 2168 to EB and MS and and DFG SCHL1930/1-2. M.R. is funded by the Deutsche Krebshilfe through a Mildred Scheel Nachwuchszentrum Grant (Grant number 70113307). SL was initially funded by a PhD Scholarship from Bayer Pharma AG (Project number 40860128)

Authors' contributions

Silke Lambing: formal analysis, investigation, writing –original draft, writing –review & editing, visualization,

Stefan Holdenrieder: conceptualization, methodology, resources,

Patrick Müller: investigation,

Christian Hagen: investigation,

Stephan Garbe: methodology, resources, writing review & editing,

Martin Schlee: methodology, resources

Jasper G. van den Boorn: investigation, methodology, supervision, project administration

Eva Bartok: formal analysis, methodology, supervision, project administration, writing – original draft, writing –review & editing, visualization

Gunther Hartmann: conceptualization, funding acquisition, methodology, project administration, resources, supervision, visualization, writing –original draft, writing –review & editing

Marcel Renn: formal analysis, investigation, methodology, project administration, supervision, writing –original draft, writing –review & editing, visualization

Acknowledgements

We thank Meghan Campbell for her critical reading of this manuscript. We thank Daniel Hinze for providing us with CRISPR gRNA/Cas9 plasmids targeting p53. We thank Jennifer Landsberg for her helpful discussion of the project.

Conflict of interest

M.S and G.H. are inventors on a patent covering synthetic RIG-I ligand. MR and GH were co-founders of Rigontec GmbH.

References

1 Esfahani K, Roudaia L, Buhlaiga N, *et al.* A review of cancer immunotherapy: From the past, to the present, to the future. *Current Oncology* 2020;**27**:87–97. doi:10.3747/co.27.5223

2 Bai L, Li W, Zheng W, *et al.* Promising targets based on pattern recognition receptors for cancer immunotherapy. *Pharmacological Research* 2020;**159**:105017. doi:10.1016/j.phrs.2020.105017

3 Junt T, Barchet W. Translating nucleic acid-sensing pathways into therapies. Nature Reviews Immunology. 2015;**15**:529–44. doi:10.1038/nri3875

4 Goubau D, Schlee M, Deddouche S, *et al.* Antiviral immunity via RIG-I-mediated recognition of RNA bearing 5′-diphosphates. *Nature* 2014;**514**:372–5. doi:10.1038/nature13590

5 Hornung V, Ellegast J, Kim S, *et al.* 5′-Triphosphate RNA Is the Ligand for RIG-I. *Science* 2006;**314**:994–7. doi:10.1126/science.1132505

6 Schlee M, Roth A, Hornung V, *et al.* Recognition of 5′ Triphosphate by RIG-I Helicase Requires Short Blunt Double-Stranded RNA as Contained in Panhandle of Negative-Strand Virus. *Immunity* 2009;**31**:25–34. doi:10.1016/j.immuni.2009.05.008

7 Besch R, Poeck H, Hohenauer T, *et al.* Proapoptotic signaling induced by RIG-I and MDA-5 results in type I interferon-independent apoptosis in human melanoma cells. 2009;**119**. doi:10.1172/JCI37155.The

8 Poeck H, Besch R, Maihoefer C, *et al.* 5′-triphosphate-siRNA: turning gene silencing and Rig-I activation against melanoma. *Nature Medicine* 2008;**14**:1256–63. doi:10.1038/nm.1887

9 Kroemer G, Galluzzi L, Kepp O, *et al.* Immunogenic Cell Death in Cancer Therapy. *Annual Review of Immunology* 2013;**31**:51–72. doi:10.1146/annurev-immunol-032712-100008

10 Bek S, Stritzke F, Wintges A, *et al.* Targeting intrinsic RIG-I signaling turns melanoma cells into type I interferon-releasing cellular antitumor vaccines. *OncoImmunology* 2019;**8**:1–9. doi:10.1080/2162402X.2019.1570779

11 Castiello L, Zevini A, Vulpis E, *et al.* An optimized retinoic acid-inducible gene I agonist M8 induces immunogenic cell death markers in human cancer cells and

dendritic cell activation. *Cancer Immunology, Immunotherapy* 2019;**68**:1479–92. doi:10.1007/s00262-019-02380-2

12 Duewell P, Steger a, Lohr H, *et al.* RIG-I-like helicases induce immunogenic cell death of pancreatic cancer cells and sensitize tumors toward killing by CD8(+) T cells. *Cell death and differentiation* 2014;**21**:1–13. doi:10.1038/cdd.2014.96

13 van den Boorn JG, Hartmann G. Turning tumors into vaccines: co-opting the innate immune system. *Immunity* 2013;**39**:27–37. doi:10.1016/j.immuni.2013.07.011

14 Baskar R, Lee KA, Yeo R, *et al.* Cancer and Radiation Therapy: Current Advances and Future Directions. *International Journal of Medical Sciences* 2012;**9**:193–9. doi:10.7150/ijms.3635

15 Hallahan DE, Spriggs DR, Beckett MA, *et al.* Increased tumor necrosis factor alpha mRNA after cellular exposure to ionizing radiation. *Proceedings of the National Academy of Sciences of the United States of America* 1989;**86**:10104–7.http://www.ncbi.nlm.nih.gov/pmc/articles/PMC298653/

16 Matsumura S, Wang B, Kawashima N, *et al.* Radiation-Induced CXCL16 Release by Breast Cancer Cells Attracts Effector T Cells. *The Journal of Immunology* 2008;**181**:3099 LP – 3107.http://www.jimmunol.org/content/181/5/3099.abstract

17 Marcus A, Mao AJ, Lensink-Vasan M, *et al.* Tumor-Derived cGAMP Triggers a STING-Mediated Interferon Response in Non-tumor Cells to Activate the NK Cell Response. *Immunity* 2018;**49**:754-763.e4. doi:10.1016/j.immuni.2018.09.016

18 Schadt L, Sparano C, Schweiger NA, *et al.* Cancer-Cell-Intrinsic cGAS Expression Mediates Tumor Immunogenicity. *Cell Reports* 2019;**29**:1236-1248.e7. doi:10.1016/j.celrep.2019.09.065

19 Apetoh L, Ghiringhelli F, Tesniere A, *et al.* Toll-like receptor 4-dependent contribution of the immune system to anticancer chemotherapy and radiotherapy. *Nature Medicine* 2007;**13**:1050–9. doi:10.1038/nm1622

20 Golden EB, Frances D, Pellicciotta I, *et al.* Radiation fosters dose-dependent and chemotherapy-induced immunogenic cell death. *OncoImmunology* 2014;**3**. doi:10.4161/onci.28518

21 Ohshima Y, Tsukimoto M, Takenouchi T, *et al.* γ-Irradiation induces P2X7 receptor-dependent ATP release from B16 melanoma cells. *Biochimica et Biophysica Acta - General Subjects* 2010;**1800**:40–6. doi:10.1016/j.bbagen.2009.10.008

22 Hauser SH, Calorini L, Wazer DE, *et al.* Radiation-enhanced expression of major histocompatibility complex class I antigen H-2Db in B16 melanoma cells. *Cancer Res* 1993;**53**:1952–5.

23 Reits E a, Hodge JW, Herberts C a, *et al.* Radiation modulates the peptide repertoire, enhances MHC class I expression, and induces successful antitumor immunotherapy. *The Journal of experimental medicine* 2006;**203**:1259–71. doi:10.1084/jem.20052494

24 Gameiro SR, Jammeh ML, Wattenberg MM, *et al.* Radiation-induced immunogenic modulation of tumor enhances antigen processing and calreticulin exposure, resulting in enhanced T-cell killing. *Oncotarget* 2014;**5**:403–16. doi:10.18632/oncotarget.1719

25 Obeid M, Panaretakis T, Joza N, *et al.* Calreticulin exposure is required for the immunogenicity of γ-irradiation and UVC light-induced apoptosis. Cell Death and Differentiation. 2007;**14**:1848–50. doi:10.1038/sj.cdd.4402201

26 Kang J, Demaria S, Formenti S. Current clinical trials testing the combination of immunotherapy with radiotherapy. *Journal for ImmunoTherapy of Cancer* 2016;**4**. doi:10.1186/s40425-016-0156-7

27 Twyman-Saint Victor C, Rech AJ, Maity A, *et al.* Radiation and dual checkpoint blockade activate non-redundant immune mechanisms in cancer. *Nature* 2015;**520**:373–7. doi:10.1038/nature14292

28 Theelen WSME, Chen D, Verma V, *et al.* Pembrolizumab with or without radiotherapy for metastatic non-small-cell lung cancer: a pooled analysis of two randomised trials. *The Lancet Respiratory Medicine* 2021;**9**:467–75. doi:10.1016/S2213-2600(20)30391-X

29 Goldeck M, Schlee M, Hartmann G, *et al.* Enzymatic Synthesis and Purification of a Defined RIG-I Ligand. In: Anders HJ, Migliorini A, eds. *Innate DNA and RNA Recognition. Methods in Molecular Biology (Methods and Protocols)*. Humana Press, New York, NY 2014. 15–25. doi:https://doi.org/10.1007/978-1-4939-0882-0_2

30 Obeid M, Tesniere A, Ghiringhelli F, *et al.* Calreticulin exposure dictates the immunogenicity of cancer cell death. *Nature medicine* 2007;**13**:54–61. doi:10.1038/nm1523

31 Haluska FG, Wu H, Haluska FS, *et al.* Genetic Alterations in Signaling Pathways in Melanoma. Published Online First: 2006. doi:10.1158/1078-0432.CCR-05-2518

32 Heidegger S, Kreppel D, Bscheider M, *et al.* RIG-I activating immunostimulatory RNA boosts the efficacy of anticancer vaccines and synergizes with immune checkpoint blockade. *EBioMedicine* 2019;**41**:146–55. doi:10.1016/j.ebiom.2019.02.056

33 Whitehead KA, Langer R, Anderson DG. Knocking down barriers: Advances in siRNA delivery. *Nature Reviews Drug Discovery* 2009;**8**:129–38. doi:10.1038/NRD2742

34 Box NF, Vukmer TO, Terzian T. Targeting p53 in melanoma. *Pigment Cell & Melanoma Research* 2014;**27**:8–10. doi:10.1111/pcmr.12180

35 Olivier M, Hollstein M, Hainaut P. TP53 mutations in human cancers: origins, consequences, and clinical use. *Cold Spring Harbor perspectives in biology* 2010;**2**:a001008. doi:10.1101/cshperspect.a001008

36 Momand J, Jung D, Wilczynski S, *et al.* The MDM2 gene amplification database. *Nucleic Acids Research* 1998;**26**:3453–9. doi:10.1093/nar/26.15.3453

37 Porta C, Hadj-Slimane R, Nejmeddine M, *et al.* Interferons α and γ induce p53-dependent and p53-independent apoptosis, respectively. *Oncogene* 2005;**24**:605–15. doi:10.1038/sj.onc.1208204

38 Takaoka A, Hayakawa S, Yanai H, *et al.* Integration of interferon-α/β signalling to p53 responses in tumour suppression and antiviral defence. *Nature* 2003;**424**:516–23. doi:10.1038/nature01850

39 Yoshino H, Iwabuchi M, Kazama Y, *et al.* Effects of retinoic acid-inducible gene-i-like receptors activations and ionizing radiation cotreatment on cytotoxicity against human non-small cell lung cancer in vitro. *Oncology Letters* 2018;**15**:4697–705. doi:10.3892/ol.2018.7867

40 Domankevich V, Efrati M, Schmidt M, *et al.* RIG-1-Like Receptor Activation Synergizes With Intratumoral Alpha Radiation to Induce Pancreatic Tumor Rejection, Triple-Negative Breast Metastases Clearance, and Antitumor Immune Memory in Mice. *Frontiers in Oncology* 2020;**10**. doi:10.3389/fonc.2020.00990

41 Klug F, Prakash H, Huber PE, *et al.* Low-Dose Irradiation Programs Macrophage Differentiation to an iNOS+/M1 Phenotype that Orchestrates Effective T Cell Immunotherapy. *Cancer Cell* 2013;**24**:589–602. doi:10.1016/j.ccr.2013.09.014

42 Vanpouille-Box C, Alard A, Aryankalayil MJ, *et al.* DNA exonuclease Trex1 regulates radiotherapy-induced tumour immunogenicity. *Nature communications* 2017;**8**:15618. doi:10.1038/ncomms15618

43 Chen J, Harding SM, Natesan R, *et al.* Cell Cycle Checkpoints Cooperate to Suppress DNA- and RNA-Associated Molecular Pattern Recognition and Anti-Tumor Immune Responses. *Cell Reports* 2020;**32**. doi:10.1016/j.celrep.2020.108080

44 Gehrke N, Mertens C, Zillinger T, *et al.* Oxidative damage of dna confers resistance to cytosolic nuclease trex1 degradation and potentiates STING-dependent immune sensing. *Immunity* 2013;**39**:482–95. doi:10.1016/j.immuni.2013.08.004

45 Engel C, Brügmann G, Lambing S, *et al.* RIG-I Resists Hypoxia-Induced Immunosuppression and Dedifferentiation. *Cancer Immunology Research* 2017;**5**:455–67. doi:10.1158/2326-6066.CIR-16-0129-T

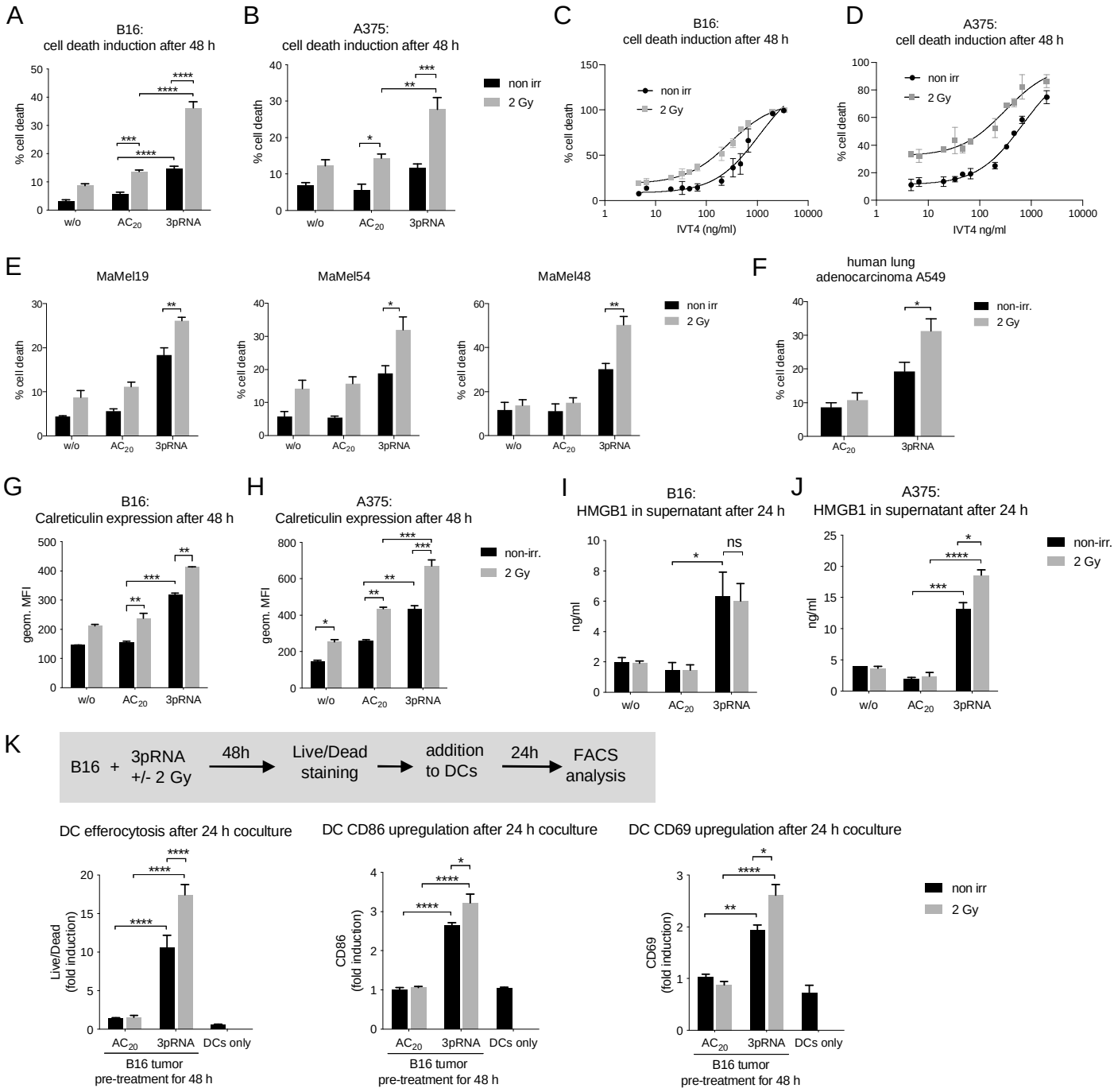

Figure 1: Irradiation enhances 3pRNA-induced immunogenic cell death in melanoma cells, as well as uptake by and co-stimulation of dendritic cells. Murine B16 and human A375 melanoma cells were transfected with 50 ng/ml 3pRNA or AC_{20} control RNA followed by 2 Gy irradiation. (A, B) 48 h later, apoptosis was measured in B16 (A) and A375 (B) cels by using Annexin V/7AAD detection by flow cytometry. (C, D) Cell death detection was repeated as described in (A, B). The dose of 3pRNA ligand was titrated in B16 (C) and A375 (D) cells to determine the EC_{50} value with and without 2 Gy, calculated by Graphpad Prism. Exemplarily titration curve shown. (E) Different human melanoma cell lines were transfected with 50 ng/ml (MaMel19) or 200 ng/ml (MaMel54, MaMel48) 3pRNA and (F) human lung carcinoma cell line A549 was transfected with 50 ng/ml 3pRNA. Cells were additionally irradiated with 0 or 2 Gy. Induction of cell death was quantified 48 h later using Annexin V/7AAD staining and flow cytometry. (G - J) Melanoma cells were transfected with 50 ng/ml 3pRNA and irradiated with 2 Gy. (G, H) After 48 h, expression of calreticulin on the cell surface was measured by flow cytometry or (I, J) after 24 h, HMGB1 concentration in the supernatant was measured by ELISA. (K) B16 cells were treated with 200 ng/ml 3pRNA and 2 Gy for 48 h, stained with fixable viability stain, and cocultured with bone-marrow-derived DCs from wildtype BL/6 mice for 24 h. DC tumor-cell uptake and activation was measured by flow cytometry. % cell death was plotted as the sum of Annexin V^+, Annexin V/7AAD^+, and $7AAD^+$ populations divided by the total number of cells. A, B, E, F, K: data are shown as mean and SEM of n=3 and I, J: n=2 independent experiments. C, D, G, H: Representative with mean and SD of n=3 independent experiments with similar results. * p<0,05; **p<0,01; ***p<0,001; ****p<0.0001. 2-way ANOVA. w/o: untreated, AC_{20}: control RNA, 3pRNA: 5'-triphosphate RNA, non-irr: non-irradiated.

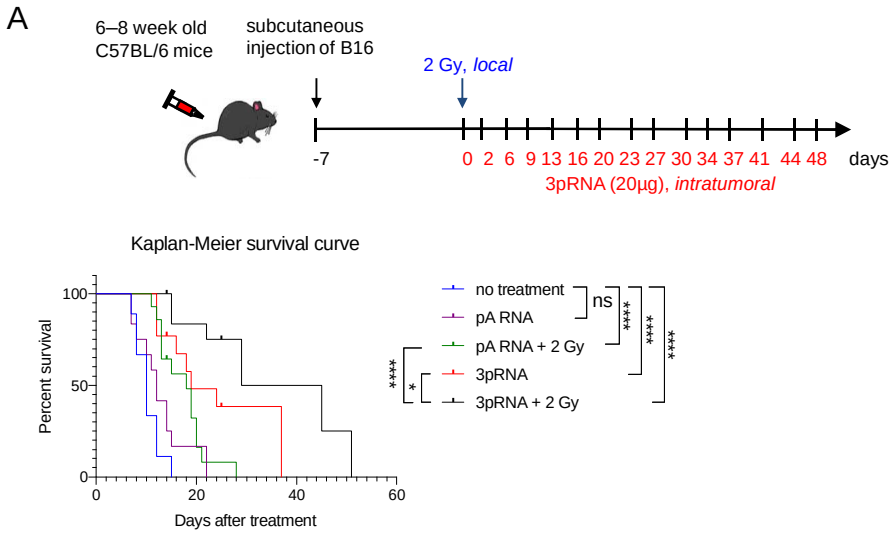

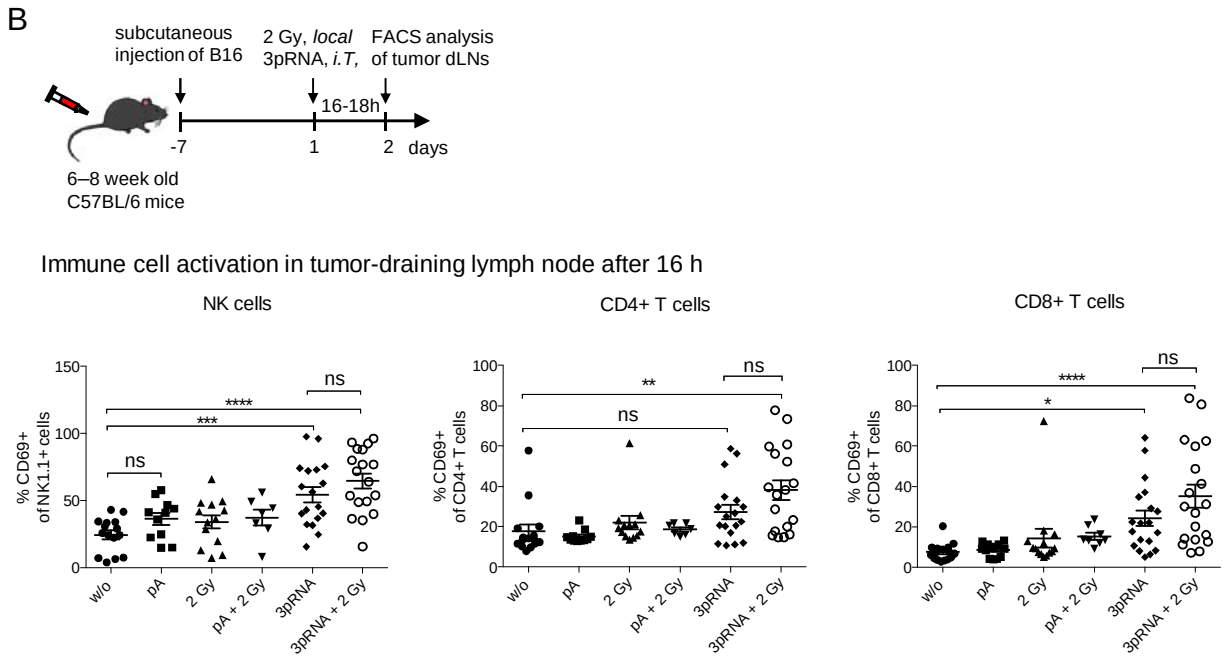

Figure 2: Concurrent irradiation and RIG-I immunotherapy prolongs the survival of melanoma-bearing mice.
(A) B16 melanoma cells, subcutaneously transplanted into C57/BL6 mice, were locally irradiated with 2 Gy, injected with 20 µg 3pRNA, 20 µg control RNA (pA) or a combination of both, as indicated, and tumor size was measured regularly over 49 days. Mice with tumors larger than 10 mm diameter were euthanized for ethical reasons. Survival rate is shown as a Kaplan−Meier curve. Summary of 3 independent experiments with 3-5 mice per group and experiment. (B) Subcutaneously transplanted B16 cells were treated as indicated and approximately 16 h later immune cells from the tumor-draining lymph nodes were analyzed for the activation marker CD69. Mean ± SEM of n = 3 with 3-5 mice per group and experiment. ns, not significant; * p<0,05; **p<0,01; ***p<0,001; ****p<0.0001; 2-Way ANOVA. w/o: untreated, pA: control RNA, 3pRNA: 5'-triphosphate RNA, non-irr: non-irradiated.

A

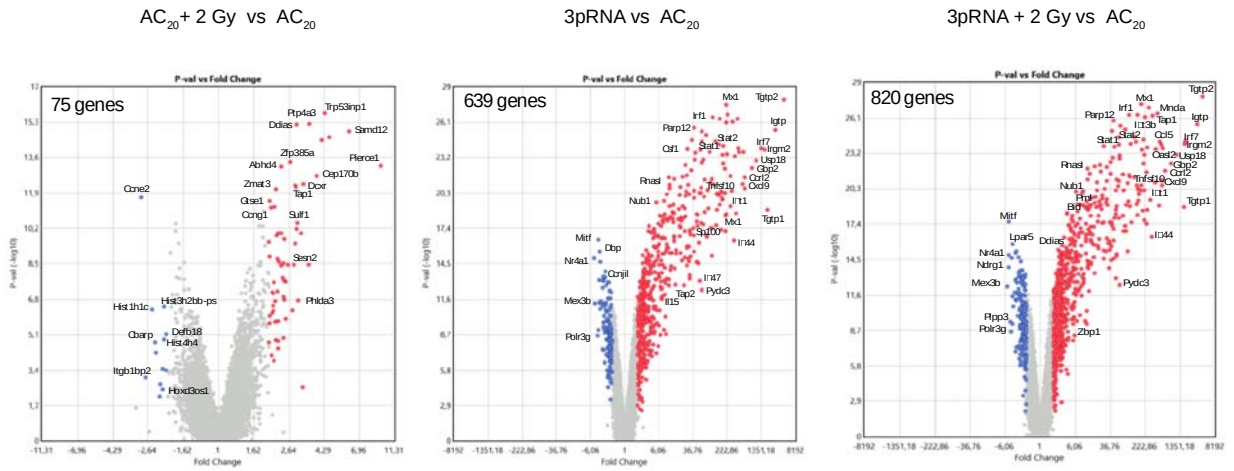

B

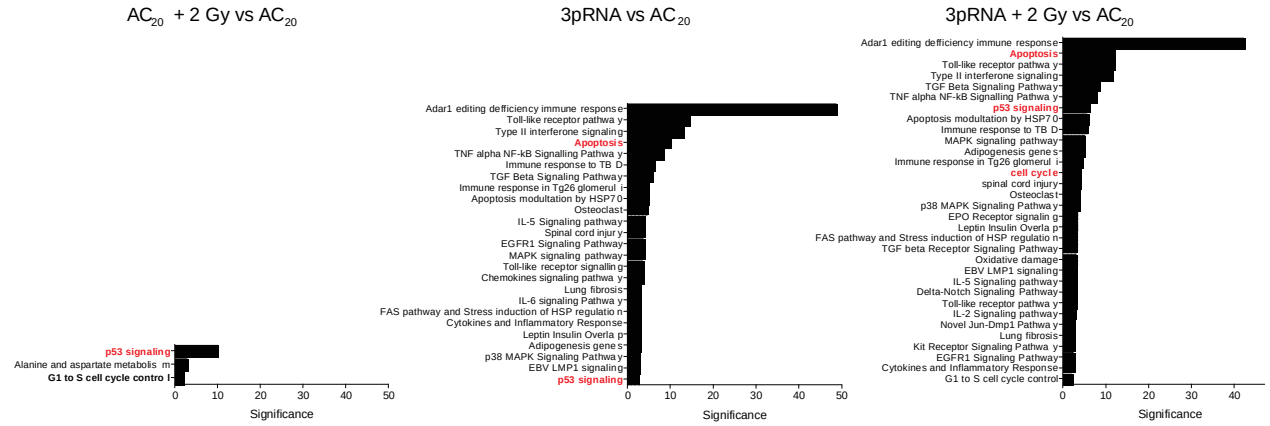

C

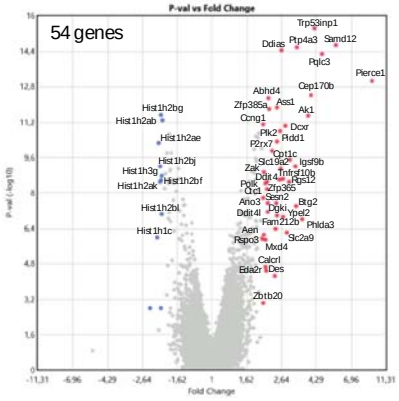

D

Figure 3: Whole-genome transcriptional analysis of B16 cells treated with the combined RIG-I radio-immunotherapy reveals activation of p53 signaling. Gene expression analysis (Affymetrix GeneChip) of B16 total RNA 6 h after stimulation with 50 ng/ml 3pRNA or AC_{20} control and 2 Gy irradiation alone or in combination. (A) Volcano plots of single treatments and combined treatment in comparison to the control-transfected B16 cells or (C) combined treatment vs. 3pRNA transfected cells. Colored data points show up- (red) or down- (blue) regulation of at least a 2 fold-change. FDR corrected p-value < 0,05 (B, D) Pathway analysis (Wikipath) of genes found in (A) and (C) using the TAC software of Thermo Fisher ordered by significance. AC_{20}: control RNA, 3pRNA: 5'-triphosphate RNA.

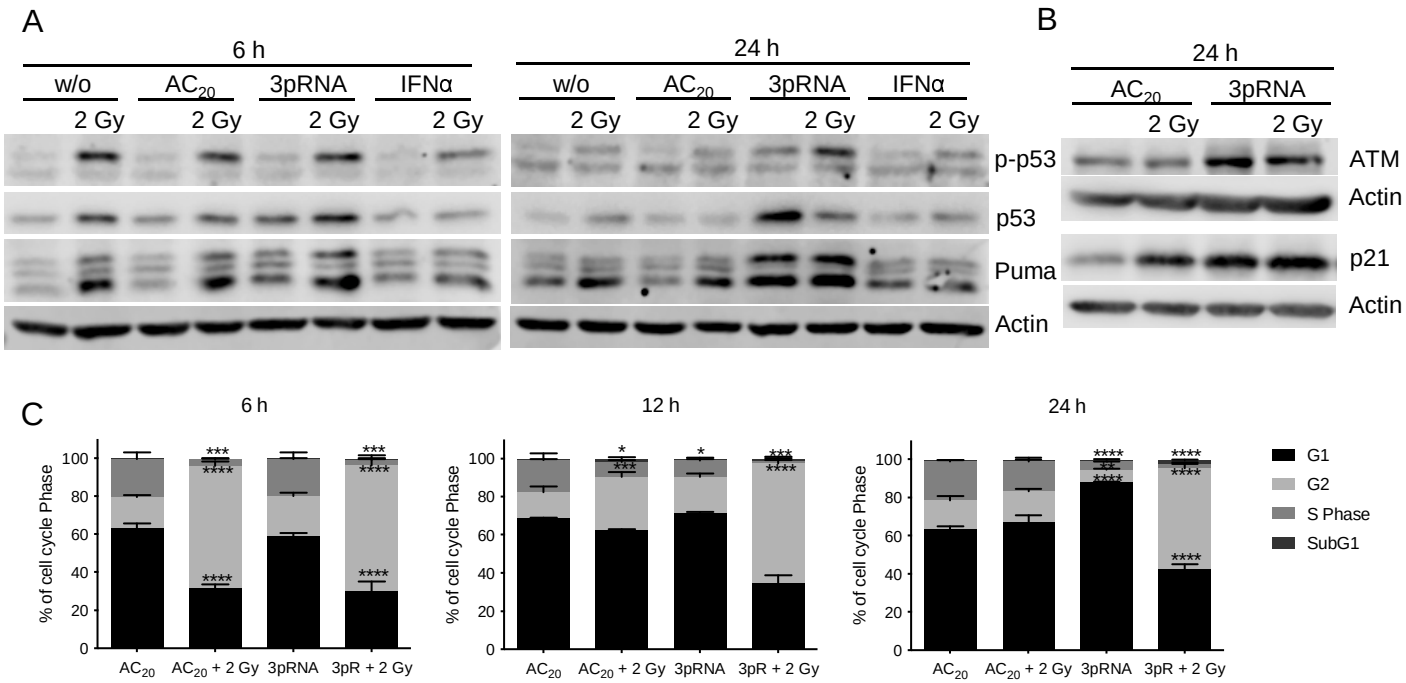

Figure 4: Combined RIG-I radio-immunotherapy induces p53 pathway activation and prolongs cell-cycle arrest. Western-blot analysis of (A) phospho- and total-p53 protein, as well as Puma expression and (B) ATM and p21 expression after irradiation with 2 Gy, transfection of 50 ng/ml 3pRNA, or the combination of both in B16 cells at the indicated time points. Actin served as a protein-loading control. (C) Flow-cytometric cell-cycle analysis of B16 cells stained with propidium iodide and treated with 50 ng/ml 3pRNA and/or 2 Gy after the indicated time points. Mean and SEM of n=2. ns, not significant; * p<0,05; **p<0,01; ***p<0,001; ****p<0.0001; two-way ANOVA. AC_{20}: control RNA, 3pRNA: 5'-triphosphate RNA.

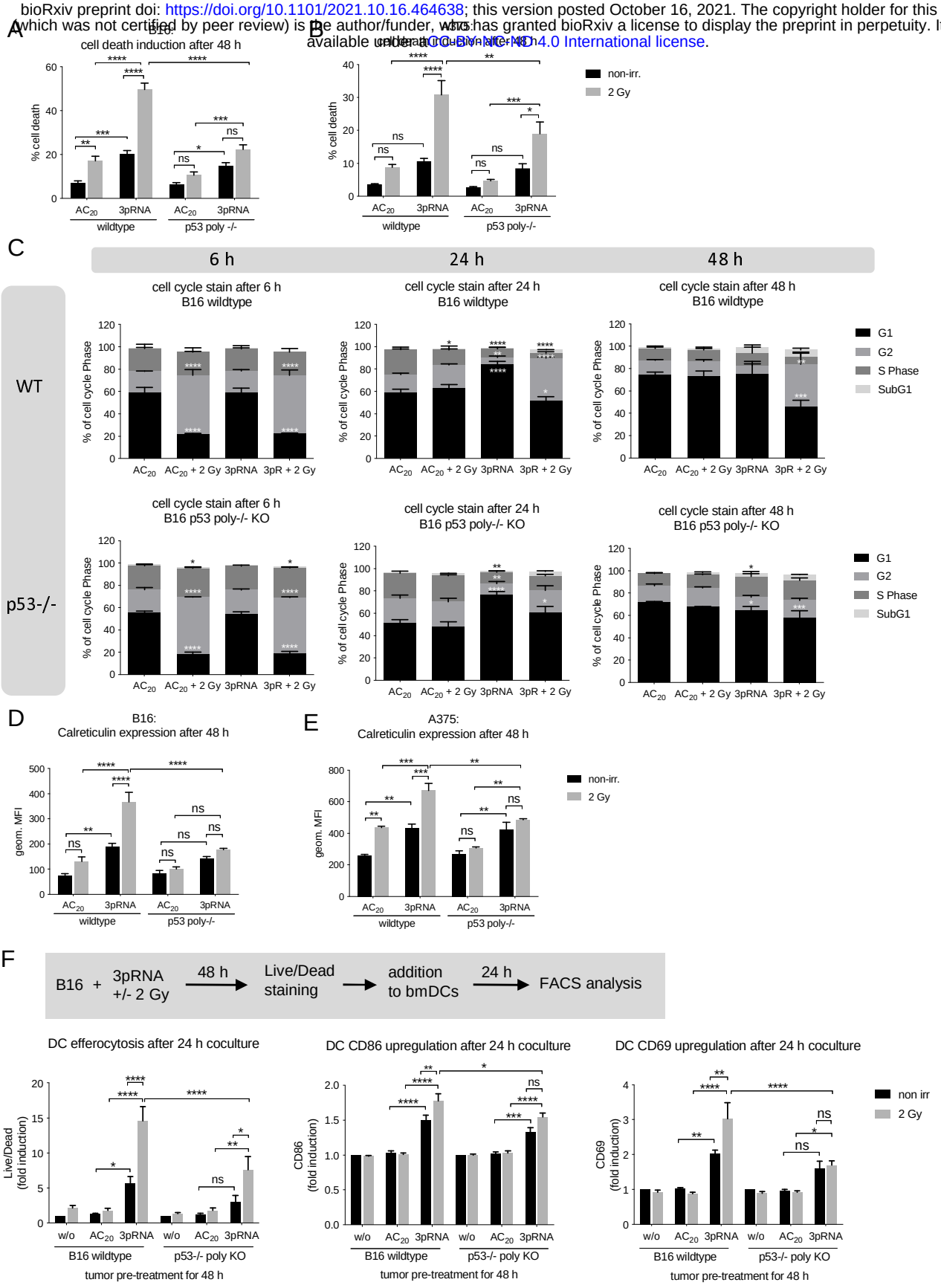

Figure 5: Knocking out p53 reduces the response of melanoma cells to combination treatment. (A–E) B16 or A375 wildtype and p53 polyclonal KO cells were transfected with 50 ng/ml 3pRNA, AC_{20} control RNA, or these in combination with 2 Gy irradiation. (A, B) Induction of cell death was quantitated via Annexin V/7AAD staining and analyzed by flow cytometry in B16 (A) and A375 (B) cells. (C) Flow-cytometric cell-cycle analysis with Hoechst 33342 at the indicated time points in B16 cells. (D, E) Surface calreticulin expression of B16 (D) and A375 (E) cells was monitored 48 h after treatment by flow cytometry. (F) B16 wildtype and p53 poly KO cells were transfected with 200 ng/ml 3pRNA and irradiated simultaneously with 0 or 2 Gy. 48 h later cells were stained by Live-Dead eFluor780 stain and cocultured with bone-marrow derived DCs overnight. Activated DCs were analyzed by flow cytometry the next day. p53 polyclonal knockout cells were generated by using the CRISPR/Cas9 system. All data are shown as the mean and SEM of n=10 (A), n=5 (D), or n=3 (B, C, E, F). * p<0,05; **p<0,01; ***p<0,001; ****p<0.0001; two-way ANOVA. ns: not significant, AC_{20}: control RNA, 3pRNA: 5'-triphosphate RNA, non-irr: non-irradiated

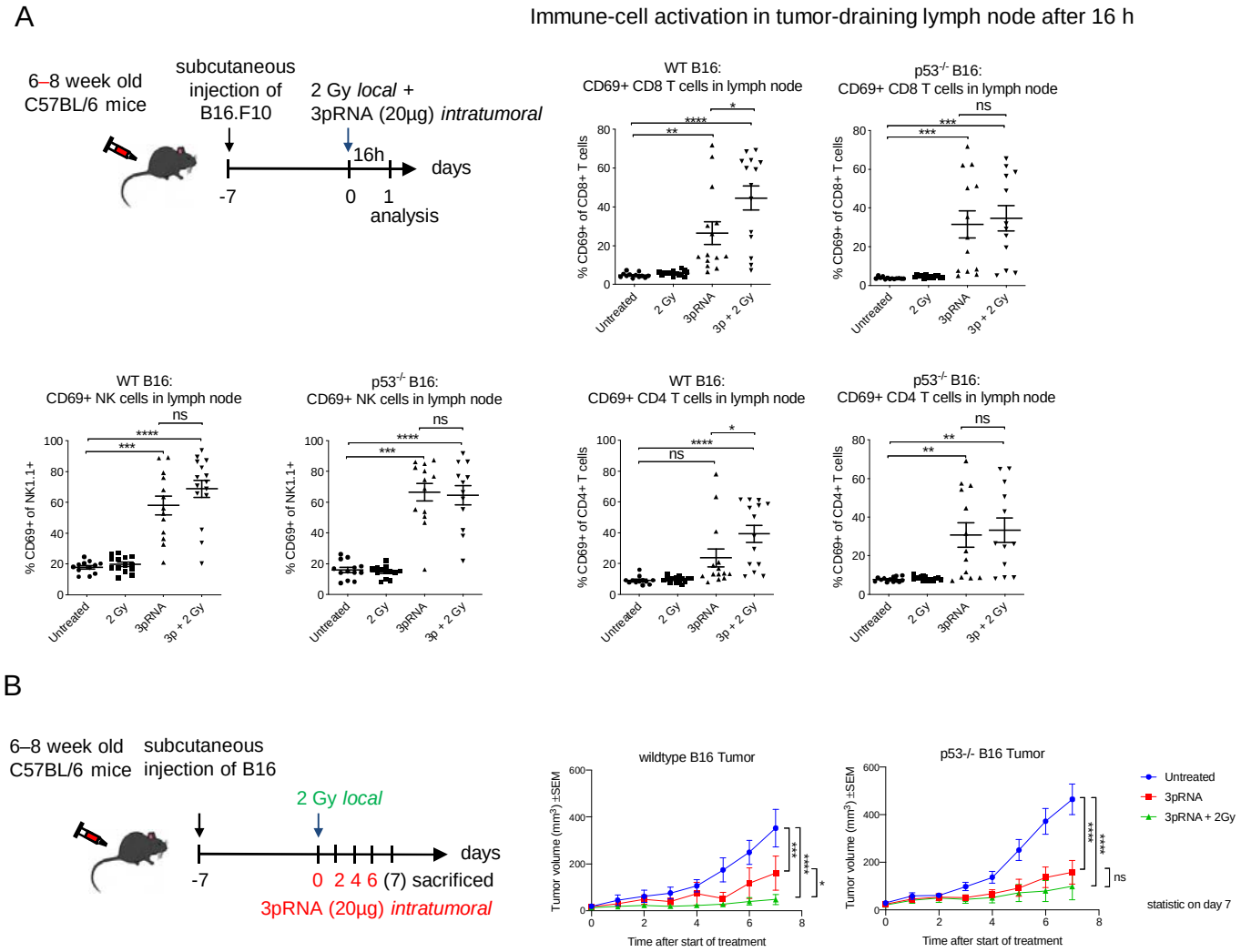

Figure 6: RIG-I immunotherapy is still effective in p53 KO melanoma, but the enhanced combinatorial efficiency with radiotherapy is abolished. (A) B16.F10 melanoma wildtype or p53 polyclonal knockout cells were subcutaneously transplanted into C57/BL6 mice and then locally irradiated with 2 Gy, injected with 20 µg 3pRNA, or a combination of both. 16 h later the mice were sacrificed. Tumor-draining lymph nodes were analyzed by flow cytometry for CD69 surface expression of activated $CD8^+$, $CD4^+$ T cells, and $NK1.1^+$ NK cells. Mean and SEM of n=3 with 3–5 mice per group and experiment. (B) Mice were treated as indicated over 7 days and the tumor size was measured daily. Mean and SEM of n = 3 with 3–5 mice per group and experiment. ns, not significant; * p<0,05; **p<0,01; ***p<0,001; ****p<0.0001; one-way ANOVA. 3pRNA: 5'-triphosphate RNA

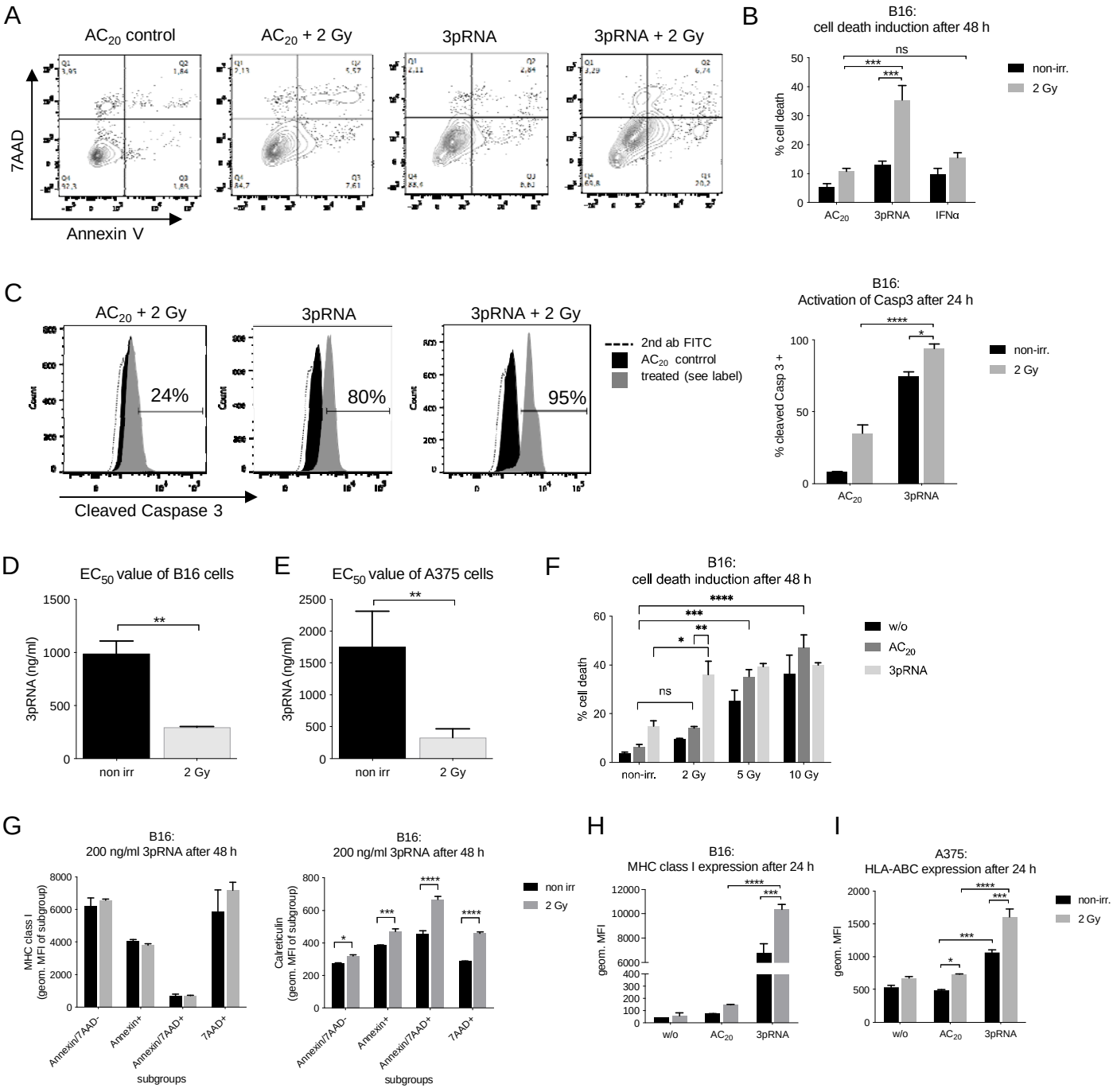

Supplementary Figure 1: Irradiation enhances 3pRNA-induced immunogenic cell death in melanoma cells, as well as uptake by and co-stimulation of dendritic cells. B16 cells were transfected with 50 ng/ml 3pRNA or AC_{20} control RNA and simultaneous irradiated with 0 or 2 Gy. (A) Gating strategy of Annexin V/7AAD staining. (B) Cells were additionally stimulated with 1000 U/ml recombinant IFNα and after 48 h, cell death was detected by Annexin V/7AAD staining. (C) Intracellular staining of activated, cleaved caspase 3 by fluorescently labeled antibody was measured after 24 h by flow cytometry. (D,E) Quantification of apoptosis induction by Annexin V/7AAD staining in B16 (D) and A375 (E) cells, 48 h after titration of 3pRNA concentration with and without 2 Gy, as shown in Fig. 1C,D. EC_{50} value of 3pRNA concentration was calculated by using GraphPad Prism. (F) B16 cells were transfected with 50 ng/ml 3pRNA and given different irradiation doses. 48 h later, cells were stained with Annexin V/7AAD and analyzed by flow cytometry. (G) Annexin V/7AAD staining after 48 h of 3pRNA (200 ng/ml) transfection and 2 Gy irradiation of B16 cells was combined with MHC class I and calreticulin fluorescent labeling. (H, I) MHC I expression on the surface of B16 (H) and A375 (I) cells 24 h after treatment, as detected by flow cytometry. (B−F) Mean and SEM, n=3. (G−I) Representative with mean and SD of n=3. * p<0,05; **p<0,01; ***p<0,001; ****p<0.0001; 2-way ANOVA. w/o: untreated, AC_{20}: control RNA, 3pRNA: 5'-triphosphate RNA, non-irr: non-irradiated.

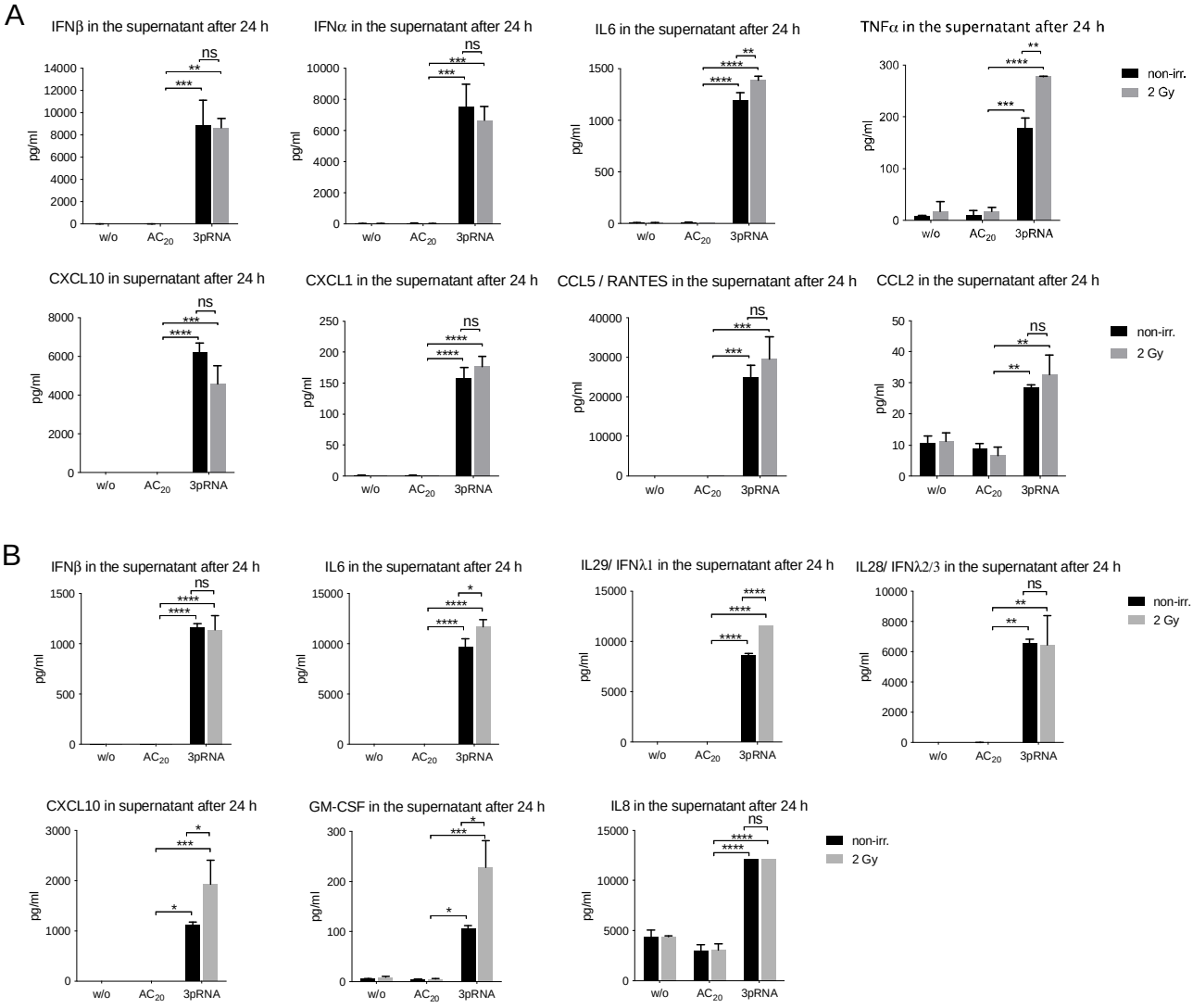

Supplementary Figure 2: 2 Gy irradiation has only minor influence on 3pRNA-induced cytokine release.
Melanoma cells were transfected with 50 ng/ml 3pRNA or AC_{20} control RNA and simultaneously irradiated with 0 or 2 Gy. Supernatants were collected 24 h after treatment of B16 (A) and A375 (B) cells, and were analyzed by flow cytometric multiplex analysis to detect different cytokines and chemokines. Shown is the mean and SD of one experiment with biological replicates measured in technical replicates. Not detected: B16 (A): IL10, GM-CSF, IL1b, IFNg, IL12p70 A375 (B): TNFa, IFNa2, IL10, IL1b, IFNg, IL12p70 * p<0,05; **p<0,01; ***p<0,001; ****p<0.0001; 2-way ANOVA. w/o: untreated, AC_{20}: control RNA, 3pRNA: 5'-triphosphate RNA, non-irr: non-irradiated.

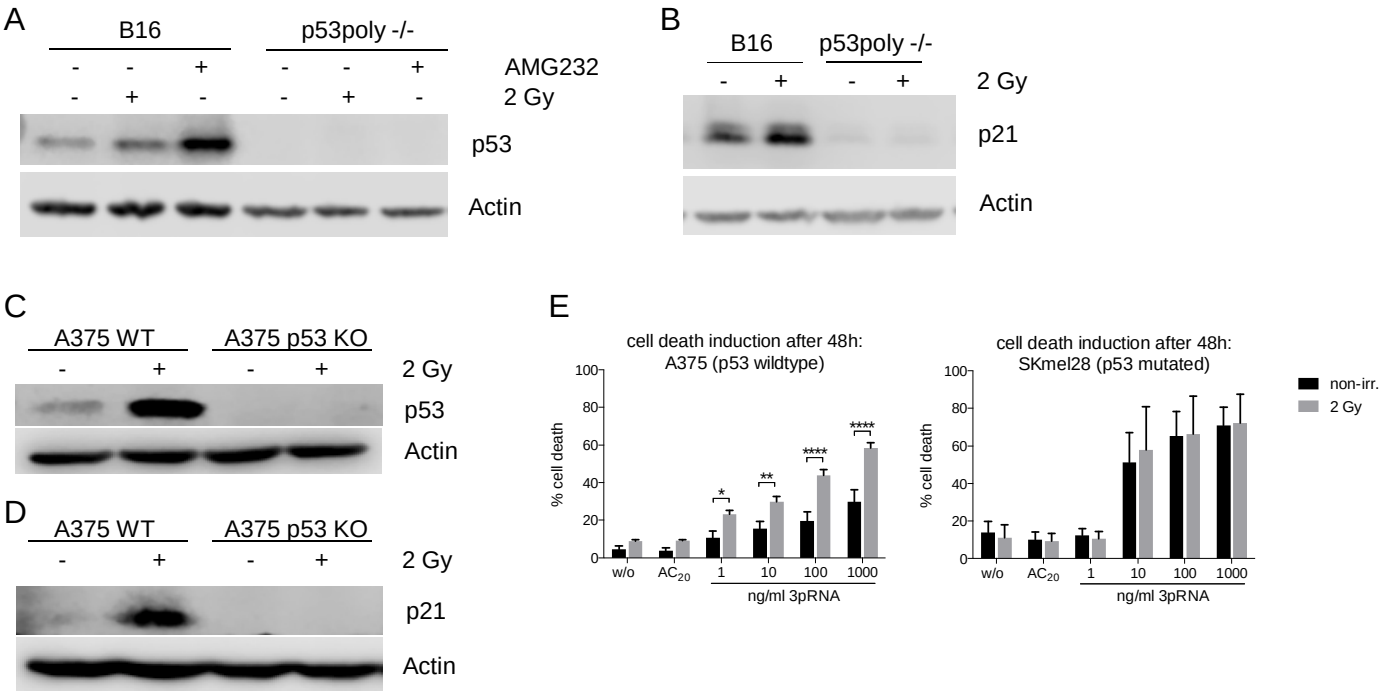

Supplementary Figure 3: Establishment of p53 polyclonal knockout melanoma and comparison of p53 wildtype and p53 mutated melanoma cells. Immunoblot analysis of p53 2 h (A, C) and p21 24 h (B, D) after irradiation with 2 Gy or treatment with 10 µM AMG232 in B16 and A375 wildtype and p53 polyclonal KO cells as indicated. Actin served as a loading control. (E) Human melanoma cell lines A375 and SKmel28 were transfected with increasing concentrations of 3pRNA and additionally irradiated with 2 Gy. Cell death was quantified 48 h later using Annexin V/7AAD staining and flow cytometry. Mean and SEM are shown from 3 independent experiments. p53 polyclonal knockout cells were generated by using the CRISPR/Cas9 system. * p<0.05; **p<0.01; ****p<0.0001; two-way ANOVA. AC_{20}: control RNA, 3pRNA: 5'-triphosphate RNA, non-irr: non-irradiated

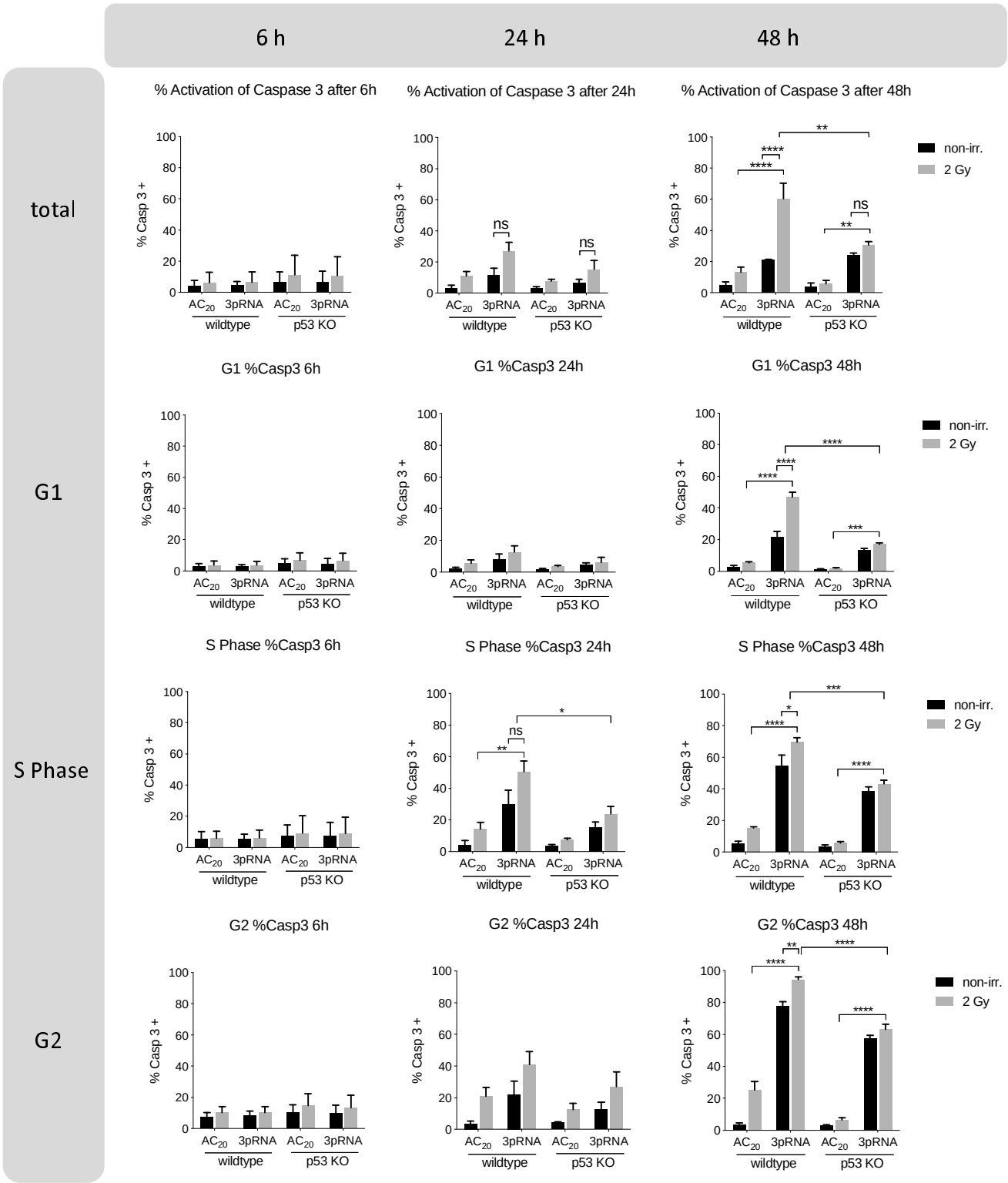

Supplementary Figure 4: Increased cell death correlates with prolonged G2/M cell cycle in combinatorial RIG-I radio-immunotherapy. Flow-cytometric cell-cycle analysis of B16 cells treated with 50 ng/ml 3pRNA and 2 Gy irradiation using genomic Hoechst 33342 stain in combination with intracellular staining with a caspase 3/7 cleavable dye at the indicated time points. p53 polyclonal knockout cells were generated by using the CRISPR/Cas9 system. * p<0,05; **p<0,01; ***p<0,001; ****p<0.0001; two-way ANOVA. ns: not significant, AC_{20}: control RNA, 3pRNA: 5'-triphosphate RNA, non-irr: non-irradiated